0254-6124/2006/26(1)-001–07 *Chin. J. Space Sci.* 空间科学学报

Feng Xueshang, Zhou Yufen, Hu Yanqi. A 3rd order WENO GLM-MHD scheme for magnetic reconnection. *Chin. J. Space Sci.*, 2006, **26**(1): 1—7

A 3rd Order WENO GLM-MHD Scheme for Magnetic Reconnection

FENG Xueshang[1] ZHOU Yufen[1,2] HU Yanqi[1,2]

[1](*Key Laboratory for Space Weather, Center for Space Science and Applied Research, Chinese Academy of Sciences, Beijing* 100080)

[2](*Graduate School, Chinese Academy of Sciences*)

Abstract A new numerical scheme of 3rd order Weighted Essentially Non-Oscillatory (WENO) type for 2.5D mixed GLM-MHD in Cartesian coordinates is proposed. The MHD equations are modified by combining the arguments as by Dellar and Dedner *et al* to couple the divergence constraint with the evolution equations using a Generalized Lagrange Multiplier (GLM). Moreover, the magnetohydrodynamic part of the GLM-MHD system is still in conservation form. Meanwhile, this method is very easy to add to an existing code since the underlying MHD solver does not have to be modified. To show the validation and capacity of its application to MHD problem modelling, interaction between a magnetosonic shock and a denser cloud and magnetic reconnection problems are used to verify this new MHD code. The numerical tests for 2D Orszag and Tang's MHD vortex, interaction between a magnetosonic shock and a denser cloud and magnetic reconnection problems show that the third order WENO MHD solvers are robust and yield reliable results by the new mixed GLM or the mixed EGLM correction here even if it can not be shown that how the divergence errors are transported as well as damped as done for one dimensional ideal MHD by Dedner *et al.*

Key words WENO scheme, MHD numerical simulation, Orszag-Tang vortex, Magnetic reconnection

1 Introduction

The WENO schemes are based on the essentially non-oscillatory (ENO) schemes, which were first developed by Harten *et al*[22] in the form of finite volume schemes. The ENO schemes are generalizations of the Total Variation Diminishing (TVD) schemes of Harten[21]. The TVD schemes typically degenerate to first-order accuracy at locations with smooth extrema while the ENO schemes maintain high-order accuracy there even in multi-spatial dimensions. Despite their high-order accuracy, ENO schemes are as capable as TVD schemes in suppressing spurious oscillations in the numerical solution. The key idea of the ENO schemes is to use the smoothest stencil among several candidates to approximate the fluxes at the cell boundaries to high order and at the same time to avoid spurious oscillations near shocks and discontinuities. The WENO schemes go one step further by taking a weighted average of all candidates. The weights are adjusted by the local smoothness of the solution so that essentially zero weights are given to non-smooth stencils while optimal weights are prescribed in smooth regions. Around the discontinuities, WENO schemes behave similarly to ENO schemes, but in the smooth regions of the solution, WENO schemes act more like an upstream centered scheme. In principle, any rth order accurate ENO scheme can be converted to a $(2r-1)$st order accurate WENO scheme. The first version of WENO schemes was developed by Liu *et al*[23] in finite volume formulation for one-dimensional conservation laws. Later,

∗ Supported by the National Natural Science Foundation of China (40374056, 40536029, 40574068), the International Collaboration Research Team Program of the Chinese Academy of Sciences
2005-02-10 收到原稿, 2005-08-20 收到修定稿

Jiang and Shu[25] presented a finite difference version of WENO schemes for multidimensional conservation laws and also optimized the accuracy of the scheme with a new weighting procedure. The finite difference WENO scheme, which has been extensively tested on multidimensional hydrodynamic problems[25], is applied here for the MHD code. As in many other modern shock capturing methods, our WENO scheme is based on the local characteristic decomposition of waves. The fluxes are first separated into each family of waves. Then they are split into positive and negative parts by either global or local Lax-Friedrichs flux splitting. Subsequently, the fluxes at the cell boundaries are constructed by the WENO approximation.

2 Divergence-Free $\nabla\cdot\boldsymbol{B}=0$ Condition and MHD Equations

Another numerical issue in the MHD calculation concerns the condition of $\nabla\cdot\boldsymbol{B}=0$. While this condition is formally ensured if it is satisfied by the initial data, the numerical truncation errors can lead to nonzero value. Since our code is of high-order accuracy in the smooth region, the errors in this condition should be small and should vanish in the limiting sense. However, across a discontinuity, the truncation error is of first order and the problem can be serious. This issue has been considered by many authors and several remedies have been tried in Ref.[1], [3], [11], [29] and [30].

One approach is to use the solution of the reduced seven-wave Riemann problem[18], using some average value for B_n on both sides, to update the seven variables other than B_n, followed by a separate step which updates B_n so as to preserve $\nabla\cdot\boldsymbol{B}=0$[12],[4]. Another approach, pioneered by Powell *et al*[11], adds terms proportional to $\nabla\cdot\boldsymbol{B}$ to the MHD system to make the one-dimensional Riemann problem nondegenerate. It is worth emphasizing that although Powell's approach maintains $\nabla\cdot\boldsymbol{B}\approx 0$ to truncation error in a multidimensional sense, in the one-dimensional Riemann problems $\nabla\cdot\boldsymbol{B}$ is comparable to $\nabla\cdot\boldsymbol{B}$. The third one has been proposed by Toth[17] in order to avoid the non conservative formulation of the source term in the Powell approach. Instead of the source term, Toth[17] has proposed a temporal and space averaging for the update of the magnetic field directly using the induction equation. Numerical experiments comparing various schemes to show the ability of keeping the $\nabla\cdot\boldsymbol{B}$ constraint have been performed by Toth[17]. It has been verified that a scheme can keep the divergence free condition by a correction method[1],[29],[30]. First, solve for the potential ϕ for the Poisson equation, $\nabla^2\phi+\nabla\cdot\boldsymbol{B}=0$, with $\boldsymbol{B}$ the updated magnetic field obtained by the WENO scheme. Then compute the corrected magnetic field as $\boldsymbol{B}^{\rm c}=\boldsymbol{B}+\nabla\phi$, for which $\nabla\cdot\boldsymbol{B}^{\rm c}=0$.

Very recently, Hans[24] proposed that upwind constrained transport on unstructured grids can effectively control the $\nabla\cdot\boldsymbol{B}=0$ constraint and pointed out that this kind of scheme can be applied to any hyperbolic system with divergence-free fields.

It should be noticed that numerical schemes in non-conservative form of MHD system can also maintain the $\nabla\cdot\boldsymbol{B}=0$ constraint to a tolerable error[5].

According to Godunov[19], Powell *et al*[11] proposed a modified form

$$\frac{\partial}{\partial t}\begin{bmatrix}\rho\\ \rho\boldsymbol{v}\\ \boldsymbol{B}\\ U\end{bmatrix}+\left\{\nabla\cdot\begin{bmatrix}\rho\boldsymbol{v}\\ \rho\boldsymbol{v}\boldsymbol{v}+(\mathcal{P})\boldsymbol{I}-\boldsymbol{B}\boldsymbol{B}\\ \boldsymbol{v}\boldsymbol{B}-\boldsymbol{B}\boldsymbol{v}\\ (U+\mathcal{P})\boldsymbol{v}-(\boldsymbol{v}\cdot\boldsymbol{B})\boldsymbol{B}\end{bmatrix}^{\rm T}\right\}^{\rm T}=-\nabla\cdot\boldsymbol{B}\begin{bmatrix}0\\ \boldsymbol{B}\\ \boldsymbol{v}\\ \boldsymbol{v}\cdot\boldsymbol{B}\end{bmatrix},\qquad(1)$$

$$\mathcal{P}=p+\frac{1}{2}\boldsymbol{B}\cdot\boldsymbol{B},$$

in which source terms proportional to $\nabla\cdot\boldsymbol{B}$ had been added to the momentum and induction and energy equations. This system was constructed by modifying the coefficient matrix in the linearized Riemann problem to include an eighth wave corresponding to passive advection of jumps in B_n with the fluid speed v_n. This is the only possibility that leaves the system invariant under the Galilean transformations $\boldsymbol{x}\to\boldsymbol{x}+\boldsymbol{v}_0t$ and $\boldsymbol{v}\to\boldsymbol{v}+\boldsymbol{v}_0$, while $\boldsymbol{B}$ and t remain unchanged.

Janhunen[10] found that the solution of the Riemann problem for Powell's system (1) for left and right states with positive fluid pressures may contain an unphysical intermediate state with negative fluid pressure. It is known that this so-called lack of positivity is a particular problem for astrophysical appli-

cations, where the contribution to the total energy from the fluid pressure is often small compared with the magnetic and possibly the kinetic energy. Thus computing the fluid pressure p from the conserved quantities $\rho, \rho\boldsymbol{v}, \boldsymbol{B}$ and U often involves the difference between two nearly equal terms. Janhunen[10] found that positivity, as well as local energy and momentum conservation, could be regained by discarding the source terms in the energy and momentum equations, so that (1) becomes

$$\frac{\partial}{\partial t}\begin{bmatrix}\rho\\ \rho\boldsymbol{v}\\ \boldsymbol{B}\\ U\end{bmatrix}+\left\{\nabla\cdot\begin{bmatrix}\rho\boldsymbol{v}\\ \rho\boldsymbol{v}\boldsymbol{v}+(\mathcal{P})\boldsymbol{I}-\boldsymbol{B}\boldsymbol{B}\\ \boldsymbol{v}\boldsymbol{B}-\boldsymbol{B}\boldsymbol{v}\\ (U+\mathcal{P})\boldsymbol{v}-(\boldsymbol{v}\cdot\boldsymbol{B})\boldsymbol{B}\end{bmatrix}^{\mathrm{T}}\right\}^{\mathrm{T}}=-\nabla\cdot\boldsymbol{B}\begin{bmatrix}0\\ 0\\ \boldsymbol{v}\\ 0\end{bmatrix}. \tag{2}$$

Dellar[9] pointed out that Powell's system (1) fails to conserve momentum and energy.

Thus, taking account of the above consideration, we will employ Janhunen's system (2) for our implementation of the numerical scheme.

In this paper we further modify the MHD equations by using the Extended Generalized Lagrange Multiplier (EGLM) formulation of the MHD system[32] as follows:

$$\frac{\partial}{\partial t}\begin{pmatrix}\rho\\ \rho\boldsymbol{v}\\ \boldsymbol{B}\\ U\\ \psi\end{pmatrix}+\left\{\nabla\cdot\begin{pmatrix}\rho\boldsymbol{v}\\ \rho\boldsymbol{v}\boldsymbol{v}+(\mathcal{P})\boldsymbol{I}-\boldsymbol{B}\boldsymbol{B}\\ \boldsymbol{v}\boldsymbol{B}-\boldsymbol{B}\boldsymbol{v}+\psi\boldsymbol{I}\\ (U+\mathcal{P})\boldsymbol{v}-(\boldsymbol{v}\cdot\boldsymbol{B})\boldsymbol{B}\\ c_{\mathrm{h}}^2\boldsymbol{B}\end{pmatrix}^{\mathrm{T}}\right\}^{\mathrm{T}}=-\nabla\cdot\boldsymbol{B}\begin{bmatrix}0\\ \boldsymbol{0}\\ \boldsymbol{v}\\ 0\\ 0\end{bmatrix}+\begin{bmatrix}0\\ \boldsymbol{0}\\ \boldsymbol{0}\\ -\boldsymbol{B}\cdot(\nabla\psi)\\ -\boldsymbol{u}\cdot(\nabla\psi)-\dfrac{c_{\mathrm{h}}^2}{c_{\mathrm{p}}^2}\psi\end{bmatrix}. \tag{3}$$

In fact, the above system can be derived by combining the arguments as used in Ref.[9], [32].

Here constants c_{h} and c_{p} are used to characterize the mixture property of hyperbolic and parabolic properties. Here, the induction equation is furthermore supplemented with a new term $\nabla\psi$ accounting for said divergence cleaning, ψ itself being an non-physical quantity which carries away any non-vanishing $\nabla\cdot\boldsymbol{B}$. For details and the eigenvalues of this system we can refer to Ref.[32].

Here, in order to consider the magnetic reconnection problem we add a source term

$$Q=[0,0,0,0,\nabla^2B_x,\nabla^2B_y,\nabla^2B_z,\boldsymbol{B}\cdot\nabla^2\boldsymbol{B}+(\mathrm{rot}\boldsymbol{B})^2,0]^{\mathrm{T}}.$$

For one-dimensional case, ENO or WENO is exactly constructed. As for the multidimensional cases, this scheme is formally extended by dimension by dimension method[26].

$$\frac{\mathrm{d}U_{i,j}}{\mathrm{d}t}=-\frac{1}{\Delta x}(\widehat{F}_{i+1/2,j}-\widehat{F}_{i-1/2,j})-\frac{1}{\Delta y}(\widehat{G}_{i,j+1/2}-\widehat{G}_{i,j-1/2})+\Delta Q_{i,j}.$$

where $\Delta Q_{i,j}$ is the centered difference at (i,j). $\widehat{F},\widehat{G}$ are the ENO approximation. For instance, $\widehat{F}$ may take the following form

$$\begin{aligned}\widehat{F}_{i+1/2,j}=&\frac{1}{12}(-F_{i-1,j}+7F_{i,j}+7F_{i+1,j}-F_{i+2,j})+\\ &\sum_{s=1}^{8}\big[-\phi_N(L_s\cdot\Delta F^{s,+}_{i-3/2,j},L_s\cdot\Delta F^{s,+}_{i-1/2,j}\cdot\\ &L_s\cdot\Delta F^{s,+}_{i+1/2,j},L_s\cdot\Delta F^{s,+}_{i+3/2,j})+\\ &\phi_N(L_s\cdot\Delta F^{s,-}_{i+5/2,j},L_s\cdot\Delta F^{s,-}_{i+3/2,j},L_s\cdot\\ &\Delta F^{s,-}_{i+1/2,j},L_s\cdot\Delta F^{s,-}_{i-1/2,j})\big]R_s.\end{aligned}$$

Here, L_s, R_s stand for the left, right eigenvector of $\dfrac{\partial F}{\partial U}$, $F^{s,\pm}_{i,j}=\dfrac{1}{2}(F_{i,j}\pm\alpha^sU_{i,j})$ with $\alpha^s=\max\limits_{0\leqslant p\leqslant N}|\lambda^s_{p,j}|$ is the global Lax-Freidrichs splitting, where $\lambda^s_{p,j}$ is the sth eigenvalue of the Jacobian $\dfrac{\partial F}{\partial U}$ evaluated at $U_{p,j}$. Similarly, we can define $\widehat{G}$.

As for the time integration, a useful 4th-order Runge-Kutta scheme is

$$\begin{aligned}U^{(1)}=&U^{(0)}+\frac{\Delta t}{2}L(U^{(0)}),\\ U^{(2)}=&U^{(1)}+\frac{\Delta t}{2}\big[-L(U^{(0)})+L(U^{(1)})\big],\\ U^{(3)}=&U^{(2)}+\frac{\Delta t}{2}\big[-L(U^{(1)})+2L(U^{(2)})\big],\\ U^{(4)}=&U^{(3)}+\frac{\Delta t}{6}\big[L(U^{(0)})+2L(U^{(1)})-4L(U^{(2)})+L(U^{(3)})\big].\end{aligned}$$

The time step size is determined every time step by

$$\Delta t=0.5\Big/\Big(\frac{\max(|v_x|+c_{\mathrm{f}}^x)}{\Delta x}+\frac{\max(|v_y|+c_{\mathrm{f}}^y)}{\Delta y}\Big).$$

The most important factor in this mixed GLM-MHD WENO scheme is how to determine the constant parameters of $c_{\rm h}$ and $c_{\rm p}$, which characterize the hyperbolic and parabolic properties of this newly formulated system. In what follows we use uniform grid meshes with Δx and Δy in x and y directions. After some tests and arguments in Ref.[32], we choose $c_{\rm h} = \max(c_{\rm f}^x, c_{\rm f}^y)$ and $c_{\rm p} = \sqrt{0.18 c_{\rm h}}$. Unfortunately, there is no general rule in selecting these paramerters.

3 2D Case: Orszag and Tang's MHD Vortex System

As an effort to apply the WENO scheme for multi-dimensional MHD problem, the Orszag and Tang's MHD vortex system[27] is calculated here. This compressible flow proposed by Orszag and Tang contains significant features of MHD turbulence, and has taken as a standard numerical test. The flow involves complex evolution due to interactions between shock waves and the vortices. The initial conditions are as follows:

$$\rho(x,y,0) = \gamma^2, \quad v_x(x,y,0) = -\sin(y),$$
$$v_y(x,y,0) = \sin(x), \quad v_z(x,y,0) = 0,$$
$$p(x,y,0) = \gamma, \quad B_x(x,y,0) = -\sin(y),$$
$$B_y(x,y,0) = \sin(2x), \quad B_z(x,y,0) = 0.$$

with $\gamma = 5/3$.

The computational domain is $[0, 2\pi] \times [0, 2\pi]$ with periodic boundary condition in both x and y directions. We use a uniform mesh of 200×200 grid nodes. We have successfully run our calculation from $t = 0$ to $t = 8$. It should be noted that GLM procedure enforces the divergence free condition of the magnetic field. This procedure maintained the integrity of the numerical solution and stabilized the calculation for long-term evolution of the MHD field. In fact, our program runs for much longer time and the calculation is stable and solution is reasonable.

For the purpose of comparison, here are shown the density contours at $t = 0.5$, $t = 2$ and $t = 3$ using the same contour level as that in Jiang and Wu[26]. Fig.1 and 2 see very complex shock structure. At $t = 2$, an intermediate shock is formed at the shock front in the region of $\pi < x < 1.5\pi$ and $0 < y < 0.75\pi$. At $t = 3$, the fast shock front in the region of $1.25\pi < x < 1.5\pi$ and $0.5\pi < y < 0.75\pi$, and a slow shock front in the region of $0.5\pi < x < \pi$ and $0.5\pi < y < 0.75\pi$. We found that our results are almost identical to those of Ref.[26] and [7].

4 Interaction Between a Magnetosonic Shock and a Denser Cloud

The next 2D example[3] is for the interaction between a magnetosonic shock and a denser cloud. The problem is of interest to the community of astrophysics and space physics.

Initially, a magnetosonic shock propagating in the x-direction with a Mach number 10, the preshock state is $(1, 1, -11.2536, 0, 0, 0, 0, 2, 2)$ for $(\rho, p, u_x, u_y, u_z, B_x, B_y, B_z)$ and the postshock state is (3.86859, 167.345, 0, 0, 0, 0, 7.73718, −7.73718). The simulation is performed in a $[0,1] \times [0,1]$ domain in which 160×160 grid cells are used. In front of the shock there is initially a circular cloud, whose center is located at $(x, y) = (0.8, 0.50)$. The radius of the cloud is 0.15. The cloud is 10 times denser than the plasma at the preshock state. An open boundary

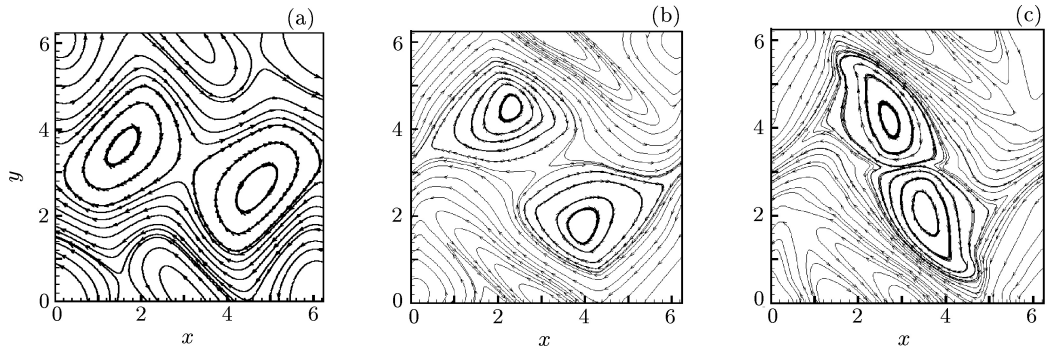

Fig.1 Density profiles of Orszag and Tang's two-dimensional MHD problem: (a) for magnetic field at $t = 0.5$, (b) for magnetic field at $t = 2$, (c) for magnetic field at $t = 3$

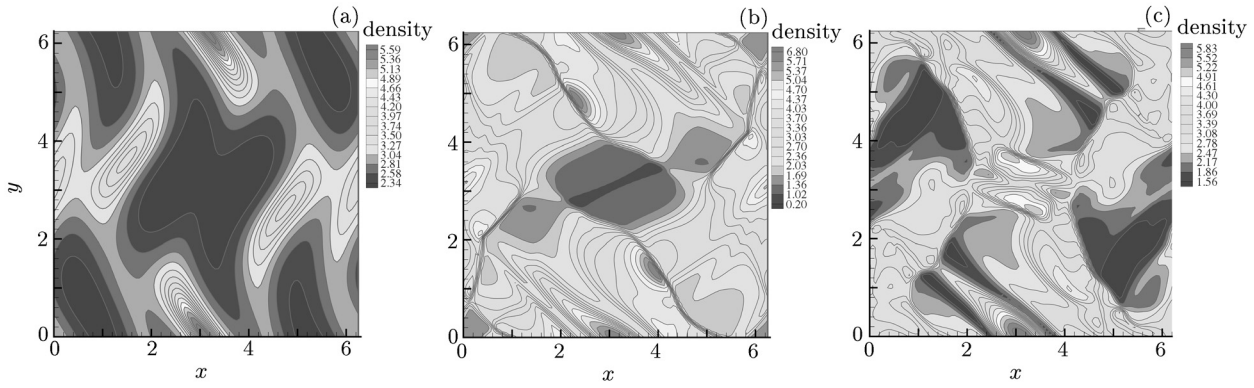

Fig.2 Density profiles of Orszag and Tang's two-dimensional MHD problem: (a) for density contours at $t = 0.5$, (b) for density contours at $t = 2$, (c) for density contours at $t = 3$

condition is used. Fig.3 shows the mass density and magnetic field lines at $t = 0.06$. The magnetic and density profiles at $t = 0.06$ are almost the same as those obtained by Dai and Woodward[3].

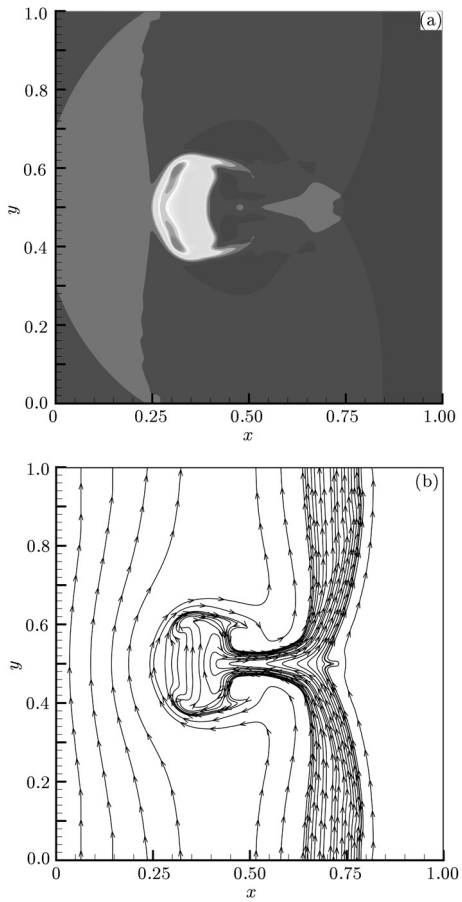

Fig.3 Interaction between a magnetosonic shock and a denser cloud: (a) for mass density contours at $t = 0.06$, (b) for magnetic field at $t = 0.06$

5 Magnetic Reconnection

The magnetic reconnection is an important physical mechanism in explaining many physical processes occurring in the solar physics and the magnetospheric physics. From induction mechanism, the magnetic reconnections could be divided into the two classes: the spontaneous and driven reconnections caused respectively by the resistive tearing mode instability and the plasma bulk moving towards the current sheet. At present, more investigations are devoted to the symmetric driven reconnection by incompressible MHD models[15],[16]. The problem whether the magnetic reconnection process can occur in interplanetary space has been discussed from both observational and numerical points of view[15],[16] and references therein.

Here, as an application of WENO scheme to magnetic reconnection problems, the same problem as in Ref.[16] is chosen for experiment. Assume that plasma cloud is centered at $(0, 6)$ with radius 1 and the computational domain is $[-8, 8] \times [-10, 8]$ with grid mesh 132×165 in x and y directions. The other parameters are the same as those in Ref.[16]. Assume that the plasma cloud with density five times higher than that of the background medium is driven with initial velocity $2v_{\rm A}$ ($v_{\rm A}$ Alfven velocity) towards the current sheet of the same form as that of Ref.[16]. In order to compare with the numerical results we further suppose that the scenario is the typical interplanetary medium: $\beta = 2.0$, $R_{\rm m} = 2000$, $N_0 = 5\,{\rm cm}^{-3}$, $T_0 = 1 \times 10^5\,{\rm K}$.

It is noted that our numerical results are almost the same as those of Ref.[16]. In Ref.[16], a poten-

tial vector magnetic field $\boldsymbol{B} = \nabla \times \boldsymbol{A}$ is used in the MHD equation and this treatment is believed to automatically satisfy magnetic field divergence-free condition during the evolutionary process. The fact that our numerical results can reproduce the very similar configuration, to some extent, shows that the mixed GLM modified MHD Eq.(3) can well keep the divergence-free condition for the magnetic field. In one dimensional ideal MHD case, Dedner *et al*[32] showed that the mixed hyperbolic/parabolic GLM ansatz offers both propagation and damping of divergence errors. In two dimensional case here, it is difficult to give a detailed discussion about how the divergence errors are transported as well as damped as done in Ref.[32].

6 Conclusion

A new WENO mixed GLM MHD numerical scheme of third order accuracy is proposed in 2.5D Cartesian case. It is significant to modify the MHD equations by coupling the divergence constraint[9] with the evolution equations using a generalized Lagrange multiplier[32]. After our modification, the magnetohydrodynamic part of the GLM-MHD system is still in conservation form by taking account of the arguments by Ref.[9] and [32]. Thus these corrections made in Ref.[32] and here may be viewed as an extension of the "divergence wave" in the ansatz of Powell *et al*[11].

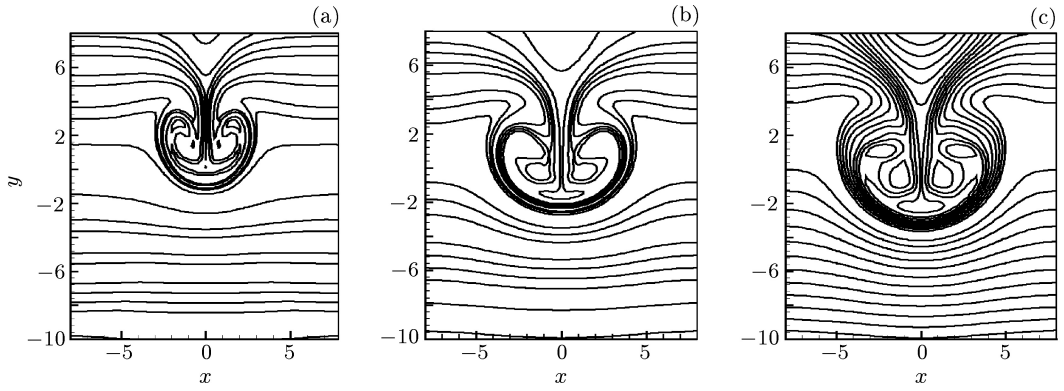

Fig.4 Magnetic field profiles of magnetic reconnection problem: (a) for magnetic field at $t = 10\tau_{\rm A}$, (b) for magnetic field at $t = 18\tau_{\rm A}$, (c) for magnetic field at $t = 26\tau_{\rm A}$

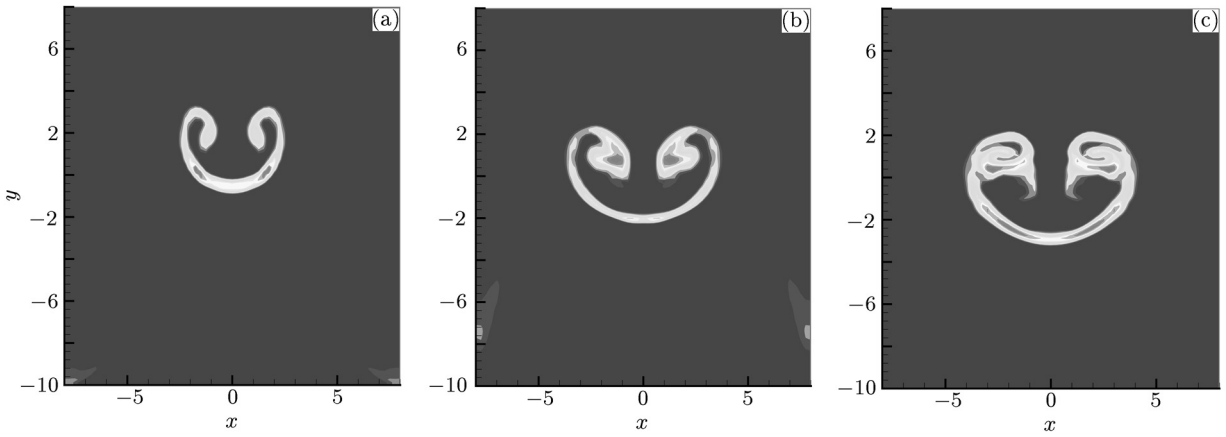

Fig.5 Density contours of magnetic reconnection problem: (a) for density at $t = 10\tau_{\rm A}$, (b) for density at $t = 18\tau_{\rm A}$, (c) for density at $t = 26\tau_{\rm A}$

The numerical tests for 2D Orszag and Tang's MHD vortex, interaction between a magnetosonic shock and a denser cloud and magnetic reconnection problems show that the third order WENO MHD solvers are robust and yield reliable results from the modified MHD Eq.(6) by well keeping the magnetic field-free condition.

By the way, we have applied this mixed GLM-MHD formulation to other problems of solar wind simulation and solar disturbances in solar-terrestrial space.

References

[1] Brackbill J U, Barnes D C. The effect of nonzero div $\boldsymbol{B}$ on the numerical solution of the magnetohydrodynamic equations. *J. Comp. Phys.*, 1980, **35**:426—430

[2] Dai W, Woodward P R. On the divergence-free condition and conservation laws in numerical simulations for supersonic magnetohydrodynamic flows. *Ap. J.*, 1998, **494**:317—335

[3] Dai W, Woodward P R. A simple finite difference scheme for multidimensional magnetohydrodynamical equations. *J. Comp. Phys.*, 1998, **142**:331—369

[4] Dai W, Woodward P R. A high-order Godunov-type scheme for shock interactions in ideal magnetohydrodynamics. *SIAM J. Sci. Comp.*, 1997, **18**(4):957—981

[5] Feng Xueshang *et al.* Numerical methods in solar wind simulations. *Space Sci. Rev.*, 2003, **107**:43—53

[6] Feng Xueshang, Wu S T, Fan Quanlin, Wei Fengsi. A class of TVD type combined numerical scheme for MHD equatiand its application to MHD numerical simulation. *Chin. J. Space Sci.*, 2002, **22**(4):316—323. in Chinese

[7] Feng Xueshang, Wei Fengsi, Zhong Dingkun. A class of Two-step TVD Maccormack type numerical scheme for MHD equations. *Chin. J. Space Sci.*, 2003, **23**(6):401—412. in Chinese

[8] Fan Quanlin, Wei Fengsi, Feng Xueshang. Start-time of magnetic reconnection in interplanetary space. *Chin. Phys. Lett.*, 2003, **20**(4):538—541

[9] Dellar P J. A note on magnetic monopoles and the one-dimensional MHD Riemann problem. *J. Comp. Phys.*, 2001, **172**:392—398

[10] Janhunen P. A positive conservative method for magnetohydrodynamics based on HLL and Roe methods. *J. Comp. Phys.*, 2000, **160**:649—661

[11] Powell K G, Roe P L, Linde T J, Gombosi T I, De Zeeuw D L. A solution-adaptive upwind scheme for ideal magnetohydrodynamics. *J. Comp. Phys.*, 1999, **154**:284—309

[12] Brio M, Wu C C. An upwind differencing scheme for the equations of ideal magnetohydrodynamics. *J. Comp. Phys.*, 1998, **75**:400—422

[13] Kulikovskiy A G, Lyubimov G A. Magnetohydrodynamics. Reading: Addison Wesley, 1965

[14] Toth G, Odstrcil D. Comparison of some flux corrected transport and total variation diminishing numerical schemes for hydrodynamic and magnetohydrodynamic problems. *J. Comp. Phys.*, 1996, **128**:82—100

[15] Wei Fengsi, Hu Qiang, Feng Xueshang, Fan Quanlin. Magnetic reconnection phenomena in interplanetary space. *Space Sci. Rev.*, 2003, **107**:107—110

[16] Wei Fengsi, Hu Qiang, Feng Xueshang. Numerical study of magnetic reconnection process near interplanetary current sheet. *Chin. Sci. Bull.*, 2001, **46**(2):111—116

[17] Toth G. The $\nabla \cdot \boldsymbol{B} = 0$ constraint in shock-capturing magnetohydrodynamics codes. *J. Comp. Phys.*, 2000, **161**:605—652

[18] Roe P L, Balsara D S. Notes on the eigensystem of magnetohydrodynamics. *SIAM J. Appl. Math.*, 1996, **56**:57—67

[19] Godunov S K. A finite difference method for the numerical computation of discontinuous solutions of the equations of fluid dynamics. *Mat. Sb.*, 1959, **47**:357—393

[20] Sweby P K. High resolution schemes using flux limiters for hyperbolic conservation laws. *SIAM J. Num. Ana.*, 1984, **21**(5):995—1011

[21] Harten A. High resolution schemes for hyperbolic conservation laws. *J. Comp. Phys.*, 1983, **49**:357—393

[22] Harten A, Engquist B, Osher S, Chakravarthy S. Uniformly high-order accurate essentially nonoscillatory schemes, III. *J. Comp. Phys.*, 1987, **71**:231—303

[23] Liu X D, Osher S, Chan T. Weighted essentially nonoscillatory schemes. *J. Comp. Phys.*, 1994, **115**:200—212

[24] Sterck H D. Multi-dimensional upwind constrained transport on unstructured grids for "shallow water" magnetohydrodynamics. *AIAA*, 2001, 2001—2623

[25] Jiang G S, Shu C W. Efficient implementation of weighted ENO schemes. *J. Comp. Phys.*, 1996, **126**: 202—228

[26] Jiang G S, Wu C C. A high-Oorder WENO finite difference scheme for the equations of ideal magneto-hydrodynamics. *J. Comp. Phys.*, 1999, **150**:561—594

[27] Orszag S A, Tang C M. Small-scale structure of two-dimensional magnetohydrodynamic turbulence. *J. Fluid. Mech.*, 1979, **90**:129—143

[28] Yee H C. A class of high resolution explicit and implicit shock-capturing methods. NASA TM-101088, 1989

[29] Zachary A L, Malagoli A, Colella P. A higher-order Godunov method for multi-dimensional ideal magnetohydrodynamics. *SIAM J. Sci. Comp.*, 1994, **15**:263—284

[30] Ryu D, Jones T W, Frank A. Numerical magnetohydrodynamics in astrophysics: Algorithm and tests for multidimensional flow. *Ap. J.*, 1995, **452**:785—796

[31] Evans C R, Hawley J F. Simulation of magnetohydrodynamic flows: A constrained transport method. *Ap. J.*, 1988, **332**:659—677

[32] Dedner A *et al.* Hyperbolic divergence cleaning for the MHD equations. *J. Comp. Phys.*, 2002, **175**:645—673